Reconstruction of a rough surface profile with an iterative method based on a rigorous direct wave scattering model

Gabriel Soriano[1], ***Slimane Arhab***[2], and ***Kamal Belkebir***[3]

[1] Institut Fresnel, DU Saint Jérôme, 13397 Marseille cedex, France, gabriel.soriano@fresnel.fr

[2] slimane.arhab@fresnel.fr

[3] kamal.belkebir@fresnel.fr

Abstract

We numerically demonstrate that an iterative inverse method based on a rigourous wave scattering model can be used to retrieve the profile of a rough interface from the complex scattering amplitude in far-field. The method of moments, that is a numerical resolution of the boundary integral equations, is chosen as direct model, so that large profiles, with tens of wavelength, can be reconstructed. The two polarization cases are addressed and finally combined. Sub-wavelength resolution is reached, especially when multiple scattering occurs.

1 Introduction

The retrieval of the roughness of an interface from its scattered field is generally treated by approximate scattering models funded on single scattering [1] and often paraxial scattering hypothesis, that can be directly inversed. The roughness in itself can be the quantity of interest, like in far-field optical profilometry [2, 3, 4, 5]. In several problems like embedded objects inversion, or through-the-wall imaging, roughness appears as a noise, since intermediate interfaces are neglected or at best, considered as planes. Now, these simplifying hypothesis cannot be assumed when high transverse resolution is sought, or on surfaces presenting small transverse dimensions, that support multiple scattering.

We investigate here, with synthetic data, the performances of a reconstruction algorithm based on a rigorous modeling of the wave-surface interaction. We show, with several simulated experiments, that the transverse resolution and axial accuracy is much better than that obtained with the classical fourier transform treatment. Contrary to the non-linear inversion approaches already proposed in [4], this algorithm is adapted to profile reconstruction and can deal with large samples (about one hundred of wavelengths).

2 Surface scattering

Like in a tomographic diffractive microscopy experiment, the surface is illuminated successively under different angles of incidence $\theta_\ell, \ell = 1, N_\ell$. For each illumination, the complex amplitude of the far-field diffracted by the surface is measured along the same various directions of observation $\theta_m, m = 1, N_m$. For simplicity, we consider two-dimensional scattering from a rough surface illuminated by time-harmonic electromagnetic beams at pulsation $\omega = kc$. In a Cartesian coordinates system (x, y, z) the invariance direction is the y-axis and the surface is described by the profile $\Gamma : z = \eta(x)$, with a normal unit vector $\hat{\mathbf{n}}$ directed toward the air $z > \eta(x)$. With a $\exp(-i\omega t)$ time dependence assumed, $\psi^{\text{inc}}(\mathbf{r}, \theta_\ell)$ is the y-component of the complex incident field of interest at point $\mathbf{r} = (x, z)$ of the incident beam centered on the illumination angle θ_ℓ. The footprint size of the beam on the profile is set by the tapering parameter g, following [6]. The total field $\psi = \psi^{\text{inc}} + \psi^{\text{sca}}$ is the sum of the incident and scattered field, and satisfies boundary conditions on Γ that depends on the polarization and the nature of the scattering medium $z < \eta(x)$. In far-field along the direction of the wavevector $\mathbf{k} = k\frac{\mathbf{r}}{r} = (k\cos\theta, k\sin\theta)$, the scattered field writes in the air as a cylindrical wave $\psi^{\text{sca}}(\mathbf{r}, \theta_\ell) \sim \frac{1+i}{4\sqrt{\pi}} \frac{e^{ikr}}{\sqrt{kr}} s(\theta_m, \theta_\ell)$ which complex amplitude is proportionnal to the so-called scattering amplitude $s(\theta_m, \theta_\ell)$, that depends on both the illumination angle θ_ℓ and the detection angle θ_m. Note that the optical intensity is classically defined as $I = |s|^2$. The direct surface scattering problem corresponds to

978-1-4244-6051-9/11/$26.00

the calculus of $s(\theta_m, \theta_\ell)$ for a given profile $z = \eta(x)$, while the inverse surface profiling is then stated as determining the surface $\eta(x)$ from the knowledge of the complex scattering amplitude $s(\theta_m, \theta_\ell)$.

When single and paraxial scattering are assumed, the scattering amplitude simply writes as $s(\theta_m, \theta_\ell) = N(\theta_m, \theta_\ell)\tilde{f}(Q_x)$ with $\tilde{f}$ the Fourier transform of function $f(x) = e^{-(x/g)^2 - 2ik\eta(x)}$ evaluated at $Q_x = k(\sin\theta - \sin\theta_\ell)$, and $N(\theta_m, \theta_\ell)$ a geometrical coefficient that depends on the boundary condition, but is independent of the roughness η. The Fraunhofer estimate of the roughness is thus obtained by reagencing the data to build $\tilde{f}(Q_x) = \frac{s(\theta_m,\theta_\ell)}{N(\theta_m,\theta_\ell)}$, then to compute the original $f(x)$ and to retrieve the height function $\eta(x) = \frac{\lambda}{4\pi}\arg f(x)$. This simple inversion technique is used in most holographic or phase microscopy experiments [5]. The transverse resolution is then easily estimated from the spatial frequency span of $\tilde{f}$ that is accessible with the given illumination and detection angles. Note that in [1], single scattering inversions of two-dimensional surfaces are performed without any paraxial approximation, but with similar results. Here, the major approximation is single scattering.

3 The nonlinear solution

If neither single scattering nor paraxial scattering are assumed, the link between the profile and the scattered field is functional and nonlinear. Following the boundary integral formalism [7] that enforces the Maxwell's equations, the scattering amplitude

$$s(\theta_m, \theta_\ell) = -\int_{\mathbf{r}\in\Gamma} \{\partial_n\psi(\mathbf{r}, \theta_\ell) + i\hat{\mathbf{n}}\cdot\mathbf{k}\psi(\mathbf{r}, \theta_\ell)\}\exp(-i\mathbf{k}\cdot\mathbf{r})\mathrm{d}\mathbf{r},\ \ \mathbf{k} = (k\sin\theta, k\cos\theta) \tag{1}$$

is related to the field ψ on Γ and to the normal derivative of the field $\partial_n\psi$. These surface unknowns satisfy the boundary integral equation

$$\frac{1}{2}\psi(\mathbf{r}, \theta_\ell) + \int_{\mathbf{r}'\in\Gamma} \partial_{n'}G(\mathbf{r}, \mathbf{r}')\psi(\mathbf{r}', \theta_\ell)\mathrm{d}\mathbf{r}' - \int_{\mathbf{r}'\in\Gamma} G(\mathbf{r}, \mathbf{r}')\partial_n\psi(\mathbf{r}', \theta_\ell)\mathrm{d}\mathbf{r}' = \psi^{\mathrm{inc}}(\mathbf{r}\in\Gamma, \theta_\ell), \tag{2}$$

with kernel $G(\mathbf{r}, \mathbf{r}') = \frac{-i}{4}\mathrm{H}_0^+(k|\mathbf{r} - \mathbf{r}'|)$ the 2D free space Green function (H_0^+ being the Hankel function of zero order and of the first kind), $\partial_{n'}G$ its normal derivate with respect to $\mathbf{r}'$, and right hand side ψ^{inc} the incident field on Γ. Solving equation (2) with boundary condition and then computing s through formula (1) can be mathematically represented by $\mathbf{F} : \eta \to s = \mathbf{F}\eta$ the direct or forward scattering nonlinear operator.

As $\mathbf{F}$ cannot be directly inversed, the inversion problem is generally recasted as an optimization problem. In this section the authors describe the Newton-Kantorovitch (NK) method [8] to solve the nonlinear functional equation $s = \mathbf{F}\eta$. The NK method iteratively builds up the solution of this equation by successively solving the forward problem and a local linear inverse problem. Now on, η is the real profile that is to be retrieved from s, and at each iteration step, an estimate η_{n+1} of the surface profile function is given by $\eta_{n+1} = \eta_n + f$, where η_n is the previous estimate and f is an update correction function. We aim here at minimizing the difference between far-field measures $\mathbf{F}\eta$ and calculus $\mathbf{F}\eta_{n+1}$. For this, we consider $\mathbf{D}$ the Fréchet derivative of nonlinear operator $\mathbf{F}$ at height η_n that is defined by

$$\mathbf{D}f = \frac{\partial}{\partial t}\mathbf{F}(\eta_n + tf)\bigg|_{t=0} = \lim_{t\to 0}\frac{\mathbf{F}(\eta_n + tf) - \mathbf{F}\eta_n}{t} \tag{3}$$

and that turns to be a linear operator. At this iterate, $\mathbf{D}f = \mathbf{F}\eta - \mathbf{F}\eta_n$ is the local linear inverse problem that we solve to determine f. Unfortunately, this equation is ill-posed and needs regularization. The authors use a zeroth-order standard Tikhonov regularization

$$\left[\mathbf{D}^\dagger\mathbf{D} + \mu^2\mathbf{I}\right] f = \mathbf{D}^\dagger(\mathbf{F}\eta - \mathbf{F}\eta_n) \tag{4}$$

where μ is the regularization parameter, $\mathbf{I}$ is the identity, and $\mathbf{D}^\dagger$ is the adjoint of linear operator $\mathbf{D}$.

In the perfectly conducting profile, the Dirichlet $\psi(\mathbf{r} \in \Gamma, \theta_\ell) = 0$ and Neumann $\partial_n \psi(\mathbf{r} \in \Gamma, \theta_\ell) = 0$ boundary conditions repectively apply in the TE ($\mathbf{E} = \psi(x,z)\hat{\mathbf{y}}$) and TM ($\mathbf{E} = \psi(x,z)\hat{\mathbf{y}}$) polarization cases. Here, following [9], operator $\mathbf{D}$ is built out of :

$$\delta s = \mathbf{D}f \Rightarrow \delta s(\theta_m, \theta_\ell) = \begin{cases} -\int_\Gamma \partial_n \psi(\mathbf{r}, \theta_\ell) \partial_n \psi(\mathbf{r}, -\theta_m) f(\mathbf{r}) \mathrm{d}\mathbf{r} & \text{TE} \\ -\int_\Gamma \{k^2 \psi(\mathbf{r}, \theta_\ell)\psi(\mathbf{r}, -\theta_m) - \partial_t \psi(\mathbf{r}, \theta_\ell)\partial_t \psi(\mathbf{r}, -\theta_m)\} f(\mathbf{r}) d\mathbf{r} & \text{TM} \end{cases} \quad (5)$$

with ∂_t the tangential derivate. Expressions for the dielectric or transmission case can also be found in [9].

4 Numerical results

Metallic optical surfaces are studied at the wavelength of $\lambda = 633\,\mathrm{nm}$. First, a rough surface with Gaussian height distribution of root mean square 60 nm and Gaussian autocorrelation function of length 100 nm is sutied in the TE case. The profile is $60\,\mu$m-long, with a beam parameter $g = 15\,\mu\mathrm{m}$ [6]. To compute the data, the profile is regularly sampled with $N = 4096$ points , while for inversion, the estimated profile only counts $N = 2048$ points. All scattered fields are computed thanks to method of moments [10] where the integral equation Eq. (2) is cast into a linear system with a full matrix of order N. Incidence and scattering angles are regularly sampled between $-45°$ and $+45°$ with a $1°$ step ($N_\ell = N_m = 91$). The numerical aperture is thus $NA = 0.71$ and single scattering analysis states that the resolution distance is $\frac{\lambda}{4\,NA} = 223\,\mathrm{nm}$. $\mathbf{F}\eta$ and $\mathbf{F}\eta_n$ are composed of $N_\ell N_m$ complex values. In its discretized form, $\mathbf{D}$ is a $N_\ell N_m$ by N rectangular matrix. The reconstruction given by the NK algorithm is accurate while that obtained under the Fraunhofer approximation clearly misses the high frequencies of the actual profile (fig. 1).

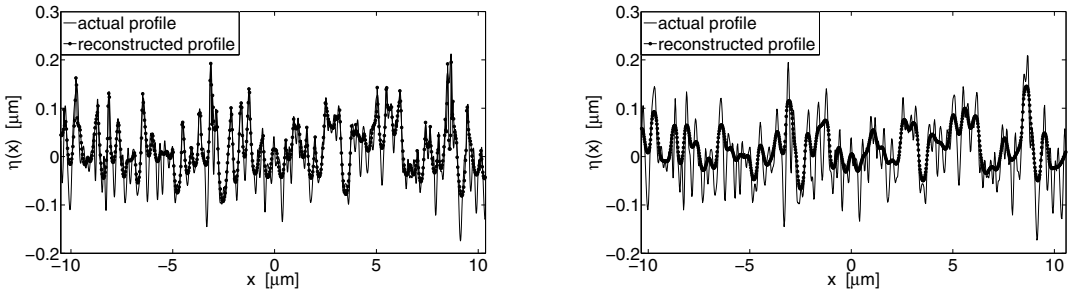

(a) (b)

Figure 1: Reconstruction at 633 nm and in the TE polarization case of a 60 μm long Gaussian rough surface metallic with rms height of 60 nm and correlation length 100 nm using (a) NK and (b) Fraunhofer approximation. Only the 20 μm central part is reported.

Next, we consider a roughness constituted by two bumps of height 140 nm separated by 200 nm (fig. 2). The incidence angle sampling step is set to $5°$, so that $N_\ell = 19$. The bumps are too close to be resolved by the Fraunhofer technique, since its resolution distance stays 223 nm ; this have been tested. It appears on figure 2a that the NK reconstruction from TE data easily beats this resolution distance. In particular, the two bumps are very precisely located. The reconstruction can be enhanced yet by combining the two polarizations cases. TE and TM data are considered, and in the iterative process, each polarization is alternatively used to produce the update correction. Here on figure 2b, the reconstruction is almost perfect, with the shape of the bumps retrieved. Such a result cannot be obtained with only TE data, even if the number of angles $N_\ell N_m$ is doubled in a way or another.

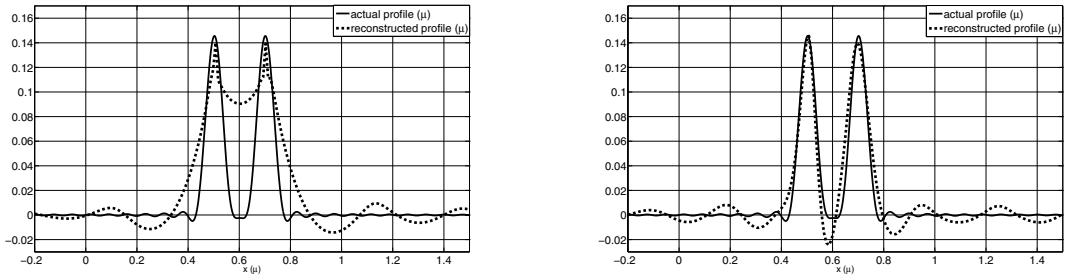

(a) (b)

Figure 2: Reconstruction at 633 nm of a metallic surface with two bumps of height 140 nm separated by 200 nm using NK (a) in the TE polarization case (b) combining the TE and TM data.

5 Conclusion

The performances of a rough profile reconstruction algorithm based on a rigorous modeling of the wave-surface interaction are far beyond the Fraunhofer resolution, but its limits mainly stay to be determined. Such an algorithm appears as a promising tool for profilometry applications. The occurence of multiple scattering, which usually plagues most imaging instruments, could even be an advantage. We have already extended this model to dielectric surfaces, and will shortly present numerical results. The next step is thus to consider two-dimensional surfaces, for which we have already developed a direct scattering model.

References

[1] R.J. Wombell and J.A. DeSanto. Reconstruction of rough-surface profiles with the Kirchhoff approximation. *Journal of the Optical Society of America A*, 8(12):1892–1897, 1991.

[2] C. J. Brakenhoff, P. Blom, and P. Barends. Confocal scanning light microscopy with high aperture immersion lenses. *J. Microsc.*, 117:219–232, 1979.

[3] Sergey A. Alexandrov, Timothy R. Hillman, Thomas Gutzler, and David D. Sampson. Synthetic aperture fourier holographic optical microscopy (vol 97, art no 168102, 2006). *Phys. Rev. Lett.*, 98(9), MAR 2 2007.

[4] G. Maire, F. Drsek, J. Girard, H. Giovannini, A. Talneau, D. Konan, K. Belkebir, P. C. Chaumet, and A. Sentenac. Experimental Demonstration of Quantitative Imaging beyond Abbe's Limit with Optical Diffraction Tomography. *Phys. Rev. Lett.*, 102:213905–4, 2009.

[5] O. Haeberlé, K. Belkebir, H. Giovannini, and A. Sentenac. Tomographic diffractive microscopy: basics, techniques and perspectives. *J. of Mod. Optics*, 57:686–699, 2010.

[6] E.I. Thorsos. The validity of the Kirchhoff approximation for rough surface scattering using a Gaussian roughness spectrum. *J. Acoust. Soc. Am*, 83(1):78–92, 1988.

[7] D. Colton and R. Kress. *Integral Equations in Scattering Theory*. Wiley-Interscience, New York, 1983.

[8] A. Roger. Newton-Kantorovitch algorithm applied to an electromagnetic inverse problem. *IEEE Transactions on Antennas and Propagation*, 29(2):232–238, 1981.

[9] A. Roger. Reciprocity theorem applied to the computation of functional derivatives of the scattering matrix. *Electromagnetics*, 2(1):69–83, 1982.

[10] L. Tsang, J. A. Kong, K. H. Ding, and C. O. Ao. *Scattering of electromagnetic waves: numerical simulations*. Wiley series in remote sensing. Wiley-Interscience, 2001.